THE ASTROPHYSICAL JOURNAL, 479:839–844, 1997 April 20

SOLID CARBONYL SULFIDE (OCS) IN DENSE MOLECULAR CLOUDS

M. E. PALUMBO
Osservatorio Astrofisico di Catania, Viale A. Doria 6, I-95125 Catania, Italy
T. R. GEBALLE
Joint Astronomy Centre, 660 N. A'ohoku Place, Hilo, HI 96720
AND
A. G. G. M. TIELENS
NASA/Ames Research Center, MS 245-3, Moffet Field, CA 94035
Received 1996 May 20; accepted 1996 October 10

ABSTRACT

An absorption feature at 2040 cm^{-1} (4.90 μm), previously observed only in W33A, has been detected toward two deeply embedded young stellar objects (YSOs), AFGL 989 and Mon R2 IRS 2. Upper limits are reported for several other YSOs and for one object located behind the Taurus Dark Cloud. We attribute this interstellar feature to solid carbonyl sulfide (OCS) embedded in icy grain mantles along the line of sight. As in the case of W33A, the best match of the newly observed features with laboratory spectra of astrophysically relevant mixtures is obtained for traces of OCS in a methanol-rich matrix. This, again, suggests the presence of independent grain mantle populations and, in particular, of a minor fraction of methanol-rich icy grain mantles in which OCS is embedded. From the strength of the absorption feature we deduce OCS column densities and OCS/H_2O ratios toward the observed objects. Taking into consideration sulfur chemistry and the origins of solid OCS, we conclude that a major fraction of the elemental sulfur is presently unaccounted for in dense molecular clouds.

Subject headings: infrared: ISM: lines and bands — ISM: clouds — ISM: molecules — line: identification — molecular processes

1. INTRODUCTION

Infrared spectra of stellar objects embedded in or located behind dense molecular clouds contain absorption features (e.g., at 3.1, 4.67, 6.0, and 6.8 μm) characteristic of simple molecules such as H_2O, CO, and CH_3OH in the solid state. These molecules are believed to be frozen in icy grain mantles (Tielens & Allamandola 1987a, Tielens 1989) formed by accretion and reaction of gas-phase species (both atoms and molecules) onto preexisting grain cores (Tielens & Hagen 1982; d'Hendecourt, Allamandola, & Greenberg 1985; Brown, Charnley, & Millar 1988). Laboratory experiments show that UV and cosmic-ray processing of these icy mantles may lead to the formation of both less volatile and more complex molecules (Lacy et al. 1984; Geballe et al. 1985; Grim & Greenberg 1987; Palumbo & Strazzulla 1993) and eventually to the formation of a complex refractory organic residue that, unlike volatile icy mantles, probably survives in the diffuse interstellar medium (Greenberg 1982; Strazzulla & Baratta 1992).

In this paper we present a search for the 2040 cm^{-1} (4.90 μm) absorption feature in several dense molecular clouds. This absorption was detected toward the deeply embedded source W33A by Larson et al. (1985) and Geballe et al. (1985), and has also been studied in this source by Palumbo, Tielens, & Tokunaga (1995). The absorption has not been detected elsewhere prior to the present work. Several carriers for the feature have been suggested. On the basis of laboratory experiments Geballe et al. (1985), attributed the observed feature to an unidentified sulfur-bearing molecule, Larson et al. (1985) proposed C_3, CN, and the overtone of the C—O stretching ($2\nu_2$) mode in CH_3OH, Grim et al. (1991) suggested CH_3OH and an unidentified absorber after comparisons with laboratory and theoretical spectra. The most recent laboratory studies and detailed comparisons of laboratory profiles with the absorption seen toward W33A by Palumbo et al. (1995) strongly indicate an identification with solid carbonyl sulfide (OCS).

2. OBSERVATIONS AND DATA REDUCTION

Infrared spectra of seven embedded young stellar objects and one background star (Elias 16) were obtained on UT 1994 October 6–7 at the United Kingdom Infrared Telescope (UKIRT) on Mauna Kea, using the facility cooled grating spectrometer, CGS4, then equipped with a 58 × 62 InSb array. The pixel angular dimension on the sky was 1.″5 × 1.″5, the slit width was 1.″5, the spectral coverage was 0.20 μm (80 cm^{-1}), and the spectral resolution was 0.0032 μm (1.3 cm^{-1}). Spectra, sampled every $\frac{1}{3}$ resolution element, were taken in a chop/nod mode with a beam separation of 30″ east-west. Typical total exposure times were 15 minutes per object. Spectra of bright stars of spectral types F and hotter (thus without CO fundamental bands) were measured at air masses matching those of the target objects and were used for ratios and flux calibration (believed to be accurate to ±30%).

In order to improve the signal-to-noise ratios, we have binned the reduced spectra, replacing each set of three adjacent points by the signal-to-noise–weighted mean value. Error bars of the mean values have been determined according to the Gaussian law of propagation of errors. The binning reduces the resolution of the spectrum by about 20%. The binned spectra are plotted in Figure 1 along with the spectrum of W33A obtained by Palumbo et al. (1995).

In most cases the error bars accurately represent the true statistical point-to-point uncertainty. However, in the case of Mon R2 IRS 2 the error bars are much larger than the point-to-point variations. This probably is related to variations in sky transparency and/or seeing, or guiding errors

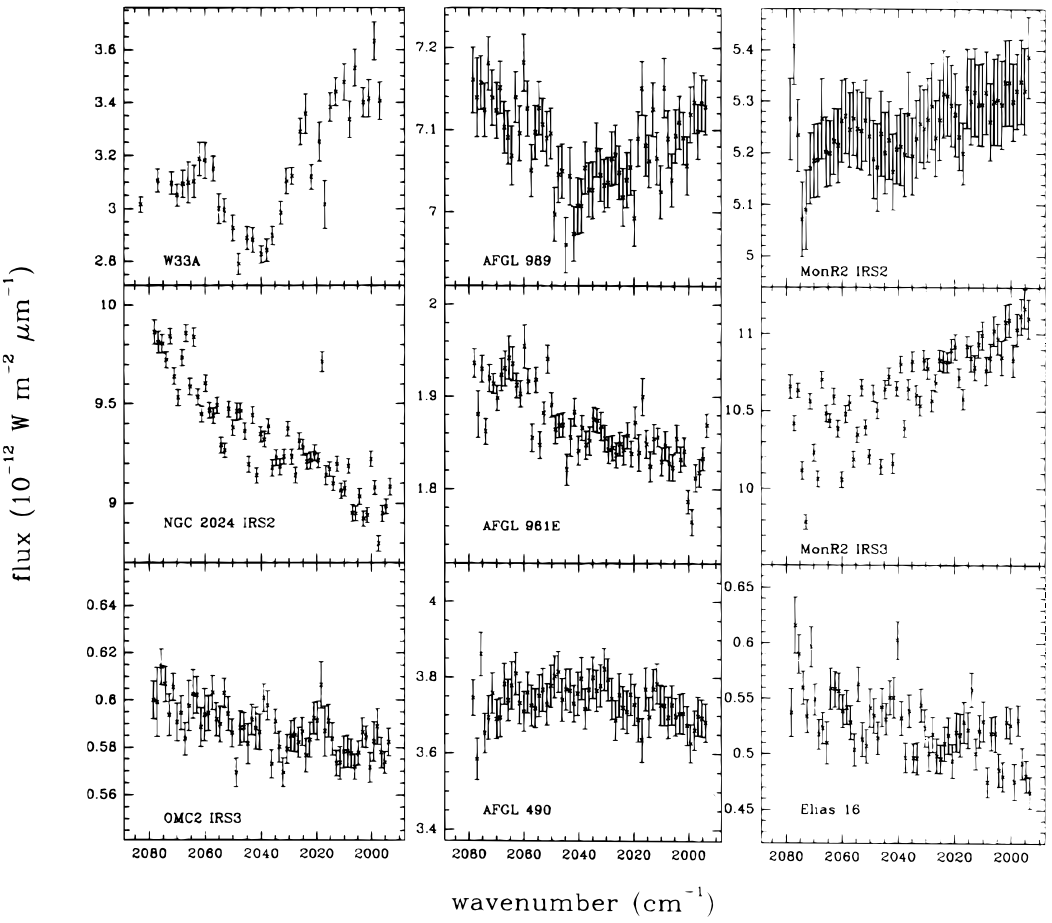

FIG. 1.—Observed spectra in the 2080–000 cm^{-1} (4.85–5.0 μm) region.

during the integration, all of which can affect the overall signal level without affecting the shape of the spectrum. In the spectrum of Mon R2 IRS 3 the error bars are smaller than the point-to-point variations. This is probably indicative of difficulties in dividing out the many deep atmospheric water lines in this wave band. The water column can be highly time-variable, and observing a calibration star at the same air mass and indeed close to the same time as the science object does not guarantee cancellation of strong water vapor lines. Mon R2 IRS 3 seems to be the only source for which this problem presented itself.

3. RESULTS

New detections of the 2040 cm^{-1} (4.90 μm) feature toward two sources, AFGL 989 and Mon R2 IRS 2, can be seen in Figure 1. The peak optical depths of the newly

TABLE 1

OPTICAL DEPTHS OF OBSERVED 2040 cm^{-1} FEATURES, SILICATES, SOLID H_2O, AND CO BANDS ALONG DIFFERENT LINES OF SIGHT

Source	τ_{OCS}	τ_{H_2O}[a]	τ_{CO}[b] "2140"	τ_{CO}[b] "2136"	τ_{sil}[a,c]	T_{ice}[d] (K)
W33A.....	0.14[e]	>5.4	1.2	0.43	5.6[f]	...
AFGL 989	0.024	1.24	0.47	0.14	2.46	<30
Mon R2 IRS 2	0.015	2.0	0.48	0.08	...	<30
AFGL 961E	<0.02	1.62	0.34	0.19	2.11	<30
AFGL 490	<0.02	0.33	0.35	0.06	2.77	...
NGC 2024 IRS 2.....	<0.01	1.0	0.46	0.08	1.7	...
Mon R2 IRS 3	<0.01	1.14[d]	...	...	4.3	≥80
OMC 2 IRS 3	<0.02	0.89	0.26	0.06	1.93	...
Elias 16.....	<0.04	1.6	1.31[g]	0.11[g]	0.66	<30

[a] Whittet & Duley 1991.
[b] Tielens et al. 1991
[c] Willner et al. 1982
[d] Smith, Sellegren, & Tokunaga 1989
[e] Palumbo et al. 1995
[f] Skinner et al. 1996
[g] Chiar et al. 1995

detected absorptions are in the range of 0.01–0.02. Upper limits, at roughly the same optical depths as those detected in the above two sources, are reported for NGC 2024 IRS 2, AFGL 961E, Mon R2 IRS 3, OMC2 IRS 3, AFGL 490, and Elias 16. All but the last are embedded protostars; Elias 16 is a late-type star located behind the Taurus Molecular Cloud.

The absorption depths of 2040 cm^{-1} features seen toward AFGL 989 and Mon R2 IRS 2 are much less than that of the feature toward W33A. However, direct comparison shows that the profiles of the features in the three sources agree within the uncertainties. Toward both sources the maximum absorption is at about 2042 ± 4 cm^{-1} (4.897 μm) with FWHM $= 23 \pm 6$ cm^{-1} (0.055 μm). In AFGL 989 the absorption profile appears to be slightly asymmetric, with a shoulder at lower frequencies. The above values compare well with the peak position and FWHM of the feature observed toward W33A. Table 1 contains estimated optical depths of the observed features toward W33A and all sources of our sample together with optical depths of absorption bands due to silicates, solid water (H_2O), and solid carbon monoxide (CO).

4. DISCUSSION

4.1. *Identification of Solid* OCS

Based both on the similarities between the newly detected absorption features and the one observed in W33A and on the laboratory studies by Palumbo et al. (1995), we attribute the 2040 cm^{-1} absorptions in AFGL 989 and Mon R2 IRS 2 to solid carbonyl sulfide (OCS). Other carriers for this band have been suggested, including the overtone of the C—O stretching mode in CH_3OH (Larson et al. 1985; Grim et al. 1991), the radicals C_3 and CN (Larson et al. 1985), and CO_3 (d'Hendecourt et al. 1996). However, all of these can be ruled out. As shown in Palumbo et al. (1995), spectra of the overtone of the C—O stretching mode in CH_3OH, both in pure icy samples and in mixtures with H_2O, do not match the observed feature. Laboratory experiments have shown that after UV photolysis of icy $CO:CH_4$ mixtures a spectral feature, tentatively attributed to the radical C_3, appears at 2027 cm^{-1}. This, however, is shifted with respect to the astronomically observed feature. CN is a radical, and its identification as the carrier of the observed 2040 cm^{-1} band is not supported by laboratory experiments. In general, besides these difficulties in fitting the observed peak position and width of the interstellar 4.9 μm band, all of these proposed identifications with radicals require fairly high radical concentrations in the interstellar ices. Such high radical concentrations are not supported by laboratory studies. Finally, although a band at 2044 cm^{-1} has been reported after UV photolysis and ion irradiation of pure CO_2 and $H_2O:CO_2$ icy mixtures (Gerakines, Schutte, & Ehrenfreund 1996; Brucato, Palumbo, & Strazzulla 1996) and attributed to solid CO_3, the FWHM of the band is only about 5 cm^{-1}. This indicates that CO_3 could only give a minor contribution to the 2040 cm^{-1} feature observed toward molecular clouds.

4.2. *Differentiation of Grain Mantles Containing Solid* OCS

Laboratory experiments (Hudgins et al. 1993; Palumbo et al. 1995) show that the wavelength of the main OCS band (due to the C=O stretch, with intrinsic band strength $A = 1.5 \times 10^{-16}$ cm molecule^{-1}) in different mixtures is close to that of the band observed toward dense molecular clouds. However, its exact profile (shape, width, frequency of peak absorption) depends on its neighbor molecules and on its temperature, and no simple relationships exist among these parameters. Moreover, Mie scattering calculations (Palumbo et al. 1995) show that the profile of the OCS band depends on the shape and size of the absorbing grain when the OCS concentration is larger than 0.05. In this case the profile is affected by surface modes, subpeaks appear, and the width of the absorption band increases. For lower OCS concentrations, laboratory bulk spectra agree very well with calculated absorption spectra of small grains. Since no subpeaks are observed in the astronomically observed profiles, the OCS concentration in interstellar grains must be less than 0.05.

In Figure 2 the spectrum observed toward AFGL 989 is compared with laboratory spectra of astrophysically relevant mixtures. The OCS band produced by traces of OCS in H_2O is shifted to higher frequencies relative to the observed feature. As shown in Palumbo et al. (1995), the bands due to traces of OCS in binary mixtures with nonpolar species (i.e., 20:1 mixtures) are also shifted to higher frequencies. Increasing the OCS abundance in the mixture causes the peak to shift to a lower wavenumber, but the bandwidth increases and no longer matches the observed feature.

Spectra of OCS embedded in $H_2O:CH_3OH$ mixtures in which H_2O is more abundant than CH_3OH and the H_2O/OCS ratio is about 100 also do not provide good fits because the OCS band is shifted with respect to the observed feature. Increasing the amount of OCS in such mixtures (e.g., $H_2O:CH_3OH:OCS = 10:1:1$) increases the width of the band beyond that of the observed feature. The match improves, however, when the CH_3OH abundance increases releative to that of H_2O. Satisfactory fits are obtained with laboratory mixtures rich in CH_3OH, namely, $CH_3OH:OCS = 20:1$ and $H_2O:CH_3OH:OCS = 3:10:1$. Similar results are obtained for Mon R2 IRS 2.

The above results imply that most of the OCS is embedded in mantles that are rich in methanol but heavily depleted in water. Such mantles must be a minor component along the line of sight since the estimated OCS/H_2O ratios are of the order of 10^{-4} (Table 2) while CH_3OH/H_2O ratios are known to range between 0.05 and 0.5 in different lines of sight (Tielens & Allamandola 1987a; Grim et al. 1991; Allamandola et al. 1992). The same conclusions have been reached for the OCS band observed toward W33A (Palumbo et al. 1995).

A number of bands of solid methanol, including the C—O stretch and CH_3 and OH stretching, bending, deformation, and rocking modes, have been identified in the lines of sight of several objects in our sample (Willner et al. 1982; Tielens & Allamandola 1987a; Grim et al. 1991; Allamandola et al. 1992; Skinner et al. 1992). Of particular interest is the C—O stretching mode observed in the spectrum of GL 2136. Laboratory studies show that the frequency of this band is sensitive to the CH_3OH/H_2O ratio of the absorbing ice. The observed frequency of 1026 cm^{-1} (9.7 μm) is characteristic of ices with high CH_3OH/H_2O ratios (>0.5), yet the CH_3OH/H_2O ratio derived from the observed column densities is only 0.1 (Skinner et al. 1992). This provides independent evidence that solid CH_3OH and solid H_2O are not well mixed in interstellar ice mantles and that some interstellar ice mantles are methanol-rich. Appar-

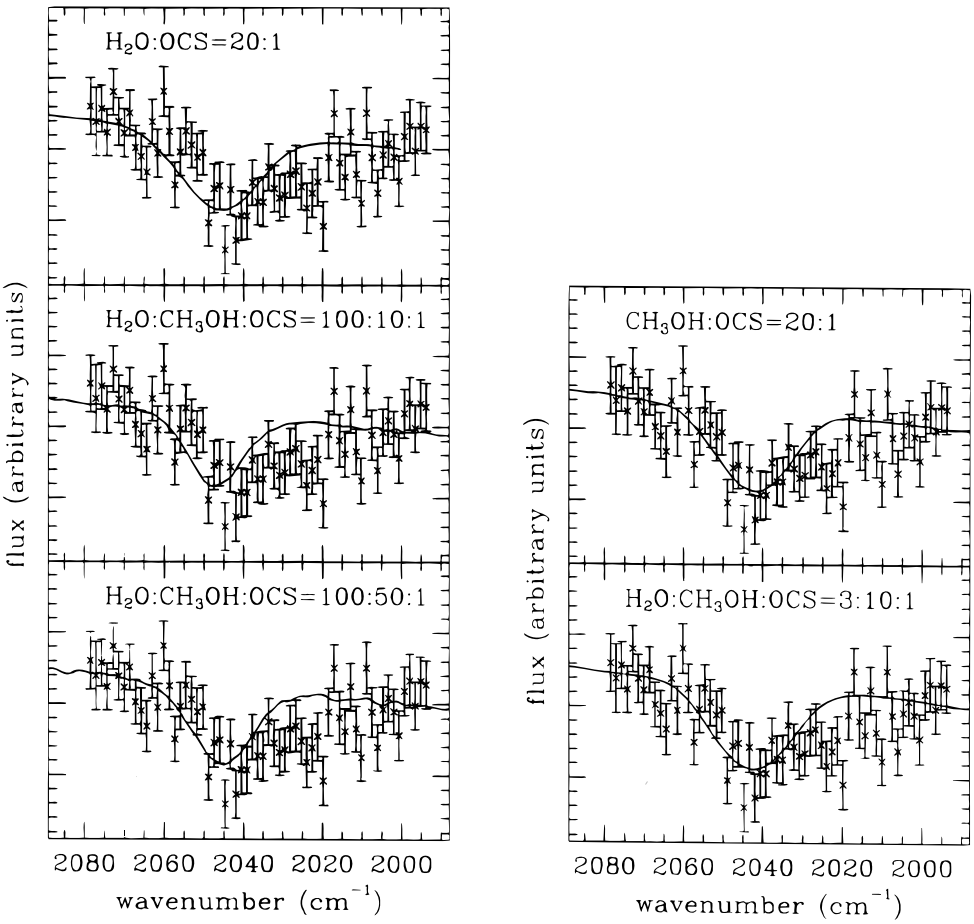

FIG. 2.—Comparisons of the observed 4.9 μm band toward AFGL 989 with laboratory spectra.

ently, whatever process causes this chemical differentiation between CH_3OH and H_2O also leads to the formation of solid OCS.

4.3. *Column Densities and Correlations*

Table 2 reports the estimated column densities of solid OCS and abundance ratios with respect to solid H_2O and CO. There are presently insufficient data on CH_3OH along the lines of sight of the sources in our sample to make meaningful comparisons with OCS. Note that solid CO is found in two independent grain components with different absorption bands, due to CO mixed in with nonpolar species and CO embedded in polar ice mantles (such as H_2O or CH_3OH-rich ices; see, e.g., Lacy et al. 1984; Tielens et al. 1991; Chiar et al. 1994, 1995; Palumbo & Strazzulla 1993).

There are no clear correlations between the strength of the 4.9 μm features and any of the other ice-band features. Table 2 shows that the $N_{ice}(OCS)/N_{ice}(H_2O)$ and $N_{ice}(OCS)/N_{polar}(CO)$ ratios vary by a factor of 2 from object to object, while the $N_{ice}(OCS)/N_{nonpolar}(CO)$ ratio varies by an order of magnitude. Also, the 4.9 μm optical depth does not seem to correlate with the total dust column density as measured by the 9.7 μm silicate optical depth.

TABLE 2

ESTIMATED SOLID OCS COLUMN DENSITY AND ABUNDANCE RATIOS

Source	$N_{ice}(OCS)$ (cm^{-2})	$\frac{N_{ice}(OCS)}{N_{ice}(H_2O)}$[a]	$\frac{N_{ice}(OCS)}{N_{nonpolar}(CO)}$[a]	$\frac{N_{ice}(OCS)}{N_{polar}(CO)}$[a]	$\frac{N_{ice}(OCS)}{N_{tot}(CO)}$	$\frac{N_{ice}(OCS)}{N_{gas}(H)}$[a]
W33A.....	2×10^{16}	4×10^{-4}	2×10^{-1}	7×10^{-2}	5×10^{-2}	7×10^{-8}
AFGL 989	2×10^{15}	1×10^{-3}	1×10^{-2}	3×10^{-2}	8×10^{-3}	2.3×10^{-8}
Mon R2 IRS 2	1.3×10^{15}	5.5×10^{-4}	8×10^{-3}	3×10^{-2}	6.5×10^{-3}	3.2×10^{-8}
AFGL 961E	$<2.6 \times 10^{15}$	$<8.8 \times 10^{-4}$	$<2 \times 10^{-2}$	$<3.5 \times 10^{-2}$	$<1 \times 10^{-2}$	$<3.5 \times 10^{-8}$
AFGL 490	$<2.6 \times 10^{15}$	$<5.3 \times 10^{-3}$	$<4 \times 10^{-2}$	$<9 \times 10^{-2}$	$<2.6 \times 10^{-2}$	$<2.6 \times 10^{-8}$
NGC 2024 IRS 2.....	$<1.3 \times 10^{15}$	$<7.2 \times 10^{-4}$	$<1 \times 10^{-2}$	$<3 \times 10^{-2}$	$<8 \times 10^{-3}$	$<2.1 \times 10^{-8}$
Mon R2 IRS 3	$<1.3 \times 10^{15}$	...	...	...	...	...
OMC 2 IRS 3	$<2.6 \times 10^{15}$	$<1.9 \times 10^{-3}$	$<2 \times 10^{-2}$	$<9 \times 10^{-2}$	$<1.6 \times 10^{-2}$	$<3.8 \times 10^{-9}$
Elias 16.....	$<5.2 \times 10^{15}$	$<1.9 \times 10^{-3}$	$<9 \times 10^{-3}$[b]	$<6.5 \times 10^{-2}$[b]	$<8 \times 10^{-3}$[b]	$<1.3 \times 10^{-7}$

[a] $N_{ice}(H_2O)$, $N_{ice}(CO)$, and $N_{gas}(H) = N(2H_2 + H)$ from Tielens et al. 1991.
[b] $N_{ice}(CO)$ from Chiar et al. 1995.

Apparently, the carrier of the 4.9 μm feature is very sensitive to the local physical conditions (or at least more so than other ice mantle components).

4.4. *The Missing Sulfur Problem*

Early low-resolution studies using *IUE* gave relatively low elemental abundances of sulfur ($\sim 4 \times 10^{-6}$) in the diffuse ISM (van Steenbergen & Shull 1988). Recent high-resolution studies using the GHRS on *HST* revealed that most of the sulfur is actually in the gas phase (1.5×10^{-5}), and, hence, sulfur is not depleted in the form of refractory grains, although only a very limited number of lines of sight have presently been studied (Sofia, Cardelli, & Savage 1994).

In molecular clouds, however, theoretical gas-phase chemistry models generally require very low elemental sulfur abundances (2×10^{-7}) in order to explain the observations of sulfur-bearing molecules (Millar & Herbst 1990), and hence support an even lower elemental sulfur abundance in molecular clouds than that measured by *IUE*.

A possible hypothesis is that the missing sulfur is locked up in icy grain mantles. However, there is no obsrvational support for this. For W33A, the abundance of solid OCS is observed to be $\sim 4 \times 10^{-4}$ relative to solid H_2O and about 10^{-7} relative to hydrogen (Table 2). Recently, a weak and broad absorption feature at 7.5 μm observed in the spectrum of W33A is attributed to solid SO_2 (Boogert et al. 1996). The derived abundance of solid SO_2 is 2×10^{-3} relative to solid H_2O and 5×10^{-7} relative to hydrogen. A weak absorption feature at 3.9 μm observed in the spectrum of W33A has been attributed to solid H_2S (Geballe et al. 1985). However, this feature and an accompanying feature at 3.85 μm (Geballe 1991) are well fitted by solid CH_3OH (Allamandola et al. 1992). Using the gas-phase integrated strength for the H_2S band (8×10^{-17} cm molecule^{-1}), we estimate a (not very restrictive) upper limit to the solid H_2S abundance of 5×10^{-7} relative to hydrogen and 2×10^{-3} relative to solid H_2O. Thus, the abundance of these sulfur-bearing molecules is not able to account for the cosmic S abundance.

There is no strong IR band that can be assigned to sulfur compounds in icy mantles. Hence, this missing sulfur, if it is in the solid state, must be in a form which has no strong IR modes or modes which are presently inaccessible. Among possible carriers are FeS, which absorbs at ~ 50 μm; MgS, which absorbs at ~ 30 μm (Begemann et al. 1994); and solid sulfur, S_8. Of these, the former two are fairly refractory dust components which might be expected to survive in the diffuse ISM. The *HST* observations of the high gas-phase elemental S abundance in the diffuse ISM suggest then that FeS and MgS are not the carriers of the missing sulfur in molecular clouds. Solid sulfur (S_8) might be formed by UV or cosmic-ray processing of sulfur-bearing molecules in icy grain mantles. Its survival in the diffuse ISM is less clear. Unfortunately, S_8 is a monovalent crystal and hence has no IR active modes. The IR spectrum of S_8 therefore shows only weak absorption features (Bernstein & Powling 1950), and its direct astronomical detection in the IR is impossible.

4.5. *The Origin of Solid* OCS

The composition of grain mantles is set by the abundances of accreting gas-phase species. Time-dependent models of gas-phase chemistry show that at early times atomic S and CS are the dominant sulfur-bearing species, with abundances of 1.5×10^{-7} and 3×10^{-8}, respectively (assuming an elemental S abundance of 2×10^{-7}; Millar & Herbst 1990). At later times, a major fraction of the atomic S has been converted into SO (abundance $\sim 10^{-7}$), while the CS abundance is largely unaffected. H_2S and OCS have calculated gaseous abundances of $\sim 10^{10}$ and 2×10^{-9}, respectively, while SO_2 can reach an abundance of 10^{-8} at late times. These results are somewhat density-dependent, with SO becoming the dominant gas-phase species at higher densities and the CS abundance decreasing by about a factor of 3 (Millar & Herbst 1990).

At 10 K, atomic S and CS are immobile on grain surfaces and, upon accretion, they will be hydrogenated by atomic H to form H_2S and H_2CS or oxidized by atomic O to form SO_2 and OCS (Tielens & Hagen 1982; Tielens & Allamandola 1987b). Thioformaldehyde (H_2CS) may react with atomic H to form methylmercaptan (CH_3SH). It has been suggested that the corresponding reactions of formaldehyde (H_2CO) are the dominant route to solid methanol (CH_3OH; Tielens & Allamandola 1987b). H_2S is unstable against attack by atomic H and O. H abstraction by atomic H leads to formation of HS, which cycles back to H_2S with another accreted H atom. Atomic H is expected to be able to tunnel through the activation barrier of ~ 850 K associated with this H-abstraction reaction (Tielens & Hagen 1982). Laboratory experiments have shown that atomic oxygen can react with H_2S at cryogenic temperatures in an Ar matrix (Smardzewski 1978). The resulting radical, either HS=O or SO, reacts with atomic O to form SO_2. SO directly accreted from the gas phase will also be oxidized by atomic oxygen. The theoretical grain-surface chemistry models by Tielens & Hagen et al. (1982) show that about half the CS accreted forms OCS, while the remainder is hydrogenated. Most of the accreted S and SO is converted into SO_2.

Thus, we expect that SO_2 is the dominant sulfur-bearing grain mantle molecule, while OCS and H_2CS have abundances a factor of 10 lower. Solid hydrogen sulfide, H_2S, is expected to have a relatively low abundance, with a solid H_2S/OCS ratio of ~ 0.1. This is in good agreement with detailed model calculations including gas-phase and grain-surface chemistry (Tielens & Hagen 1982), once allowance for recent updates (Millar & Herbst 1990) in the gas-phase chemistry scheme have been made. It also is consistent with the observations of W33A, as discussed in § 4.4.

From the interstellar chemistry considerations listed above, we draw three principal conclusions regarding the origin of solid OCS.

First, the abundance of gas-phase OCS observed in dark clouds and star-forming regons (2×10^{-9} to 10^{-8}; Irvine, Goldsmith, & Hjalmarson 1987; Ohishi, Irvine, & Kaifu 1992) is much less than that observed in the solid state (about 10^{-7}). Hence we conclude that solid OCS is formed by active grain chemistry.

Second, the solid SO_2/OCS ratio predicted by grain-surface chemistry models (~ 10) is in reasonable agreement with the observations (~ 5), lending overall support to the proposed chemical network (Tielens & Hagen 1982). Essentially, theoretical gas-phase models are in good agreement with the observed abundances of CS and SO in dark clouds (Millar & Herbst 1990), and solid OCS and SO_2 are the grain-surface oxidation productions of these species. We expect that H_2CS and/or CH_3SH also are present in interstellar grain mantles, with abundances comparable to OCS.

Third, our results indicate that solid OCS is mixed into CH_3OH-rich grain mantles. The origin of solid CH_3OH is not well understood. If CH_3OH forms from hydrogenation of CO (Tielens & Allamandola 1987b), then solid methanol would be abundantly formed only at low densities (less than $\sim 3 \times 10^4$ cm^{-3}) where the atomic H accretion rate is high. Theoretical models predict that the gas-phase CS abundance decreases with increasing density. Hence, we speculate that solid CH_3OH and OCS both trace grain mantles accreted at low densities, while mantles accreted at higher densities would have their carbons and sulfur in the form of CO and CO_2 and SO_2.

5. CONCLUSIONS

The newly detected 2040 cm^{-1} (4.9 μm) absorption bands are very similar in profile to the band detected in W33A and are attributed to solid OCS embedded in icy grain mantles along the line of sight. Comparisons of the newly discovered bands with laboratory and theoretical spectra of astrophysically relevant ice mixtures suggest that the OCS is mainly embedded in mantles with little or no water and rich in methanol. Grains with these mantles can be only a minor component along the line of sight in view of the observed ratios OCS/H_2O and CH_3OH/H_2O.

Observations and theoretical models show that sulfur is heavily depleted from the gas phase in molecular clouds. IR observations show that this sulfur is not locked up in simple sulfur-bearing molecules in icy grain mantles.

The present observations are weak evidence that solid OCS can be detected only toward certain embedded luminous protostars. It is particularly interesting that solid OCS is detected toward only one of the embedded objects in Mon R2. This suggests that the formation of solid OCS is a localized phenomenon, dependent on particular physical conditions. The apparent concentration of the OCS in a very small fraction of the grain mantles is also suggestive of this. However, as the upper limits on frozen OCS reported for most of the sources surveyed here are comparable to the column densities detected in other sources, general conclusions are premature. It is important to reach higher sensitivities and to search for the 2040 cm^{-1} feature in a larger sample of sources, including both field stars and embedded objects in different stages of their pre–main-sequence evolution, thus sampling a variety of physical conditions, in order to determine the processes that form solid OCS.

Laboratory studies have shown that the profile of the OCS band is sensitive to the composition of the mixture in which it is embedded and to the thermal history of the mixture. Further laboratory experiments mainly aimed to study the effects of UV and ion irradiation on ice samples containing sulfur-bearing molecules are to be performed. Experiments already show that solid OCS is very similar in its physical, chemical, and spectral properties to solid carbon dioxide (Sanford & Allamandola 1990; Palumbo et al. 1995).

The gas-phase and grain-surface chemistries of sulfuretted molecules imply that S, SO, and CS are important reservoirs of gas-phase sulfur. Oxidation of these species on grain surfaces will lead to SO_2 and OCS, which have both been identified in grain mantles. OCS may be mixed preferentially in CH_3OH-rich ices because both OCS and CH_3OH are formed predominantly at low gas-phase densities. Hydrogenation of the above sulfur-containing species will give rise to H_2S, H_2CS, and CH_3SH. None of these species has at present been observed in the solid state.

We wish to thank the staff of UKIRT for its support and G. Strazzulla for helpful discussions. M. E. P. acknowledges the financial support of the Italian Space Agency (ASI). The United Kingdom Infrared Telescope is operated by the Joint Astronomy Centre on behalf of the UK Particle Physics and Astronomy Research Council.

REFERENCES

Allamandola, L. J., Sandford, S. A., Tielens, A. G. G. M., & Herbst, T. M. 1992, ApJ, 399, 134
Bergemann, B., Dorschner, J., Henning, T., Mutschke, H., & Thamm, E. 1994, ApJ, 423, L71
Bernstein, H. J., & Powling, J. 1950, J. Chem. Phys., 18, 1018
Boogert, A. C. A., Schutte, W. A., Helmich, F. P., Tielens, A. G. G. M., & Wooden, D. H. 1996, A&A, in press
Brown, P. D., Charnley, S. B., & Millar, T. J. 1988, MNRAS, 231, 409
Brucato, J. R., Palumbo, M. E., & Strazzulla, G. 1996, Icarus, in press
Chiar, J. E., Adamson, A. J., Kerr, T. H., & Whittet, D. C. B. 1994, ApJ, 426, 240
———. 1995, ApJ, 455, 234
d'Hendecourt, L. B. et al. 1996, A&A, in press
d'Hendecourt, L. B., Allamandola, L. J., & Greenberg, J. M. 1985, A&A, 152, 130
Geballe, T. R. 1991, MNRAS, 251, 24
Geballe, T. R., Baas, F., Greenberg, J. M., & Schutte, W. 1985, A&A, 146, L6
Gerakines, P. A., Schutte, W. A., & Ehrenfreund, P. 1996, A&A, 312, 289
Greenberg, J. M. 1982, in Comets, ed. L. J. Wilkening (Tucson: Univ. Arizona Press), 131
Grim, R. J. M., Baas, F., Geballe, T. R., Greenberg, J. M., & Schutte, W. 1991, A&A, 243, 473
Grim, R. J. M., & Greenberg, J. M. 1987, ApJ, 321, L91
Hudgins, D. M., Sandford, S. A., Allamandola, L. J., & Tielens, A. G. G. M. 1993, ApJS, 86, 713
Irvine, W. M., Goldsmith, P. F., & Hjalmarson, A. 1987, in Interstellar Processes, ed. D. J. Hollenbach & H. A. Thronson (Dordrecht: Reidel), 561
Lacy, J. H., Baas, F., Allamandola, L. J., Persson, S. E., McGregor, P. J., Lonsdale, C. J., Geballe, T. R., & van de Bult, C. E. P. 1984, ApJ, 276, 533
Larson, H. P., Davis, D. S., Black, J. H., & Fink, U. 1985, ApJ, 299, 873
Millar, T. J., & Herbst, E. 1990, A&A, 231, 466
Ohishi, M., Irvine, W. M., Kaifu, N. 1992, in Astrochemistry of Cosmic Phenomena, ed. P. D. Singh (Dordrecht: Kluwer), 171
Palumbo, M. E., & Strazzulla, G. 1993, A&A, 269, 568
Palumbo, M. E., Tielens, A. G. G. M., & Tokunaga, A. T. 1995, ApJ, 449, 674
Sandford, S. A., & Allamandola, L. J. 1990, ApJ, 355, 357
Skinner, C. J., Justtanont, K., Tielens, A. G. G. M., Barlow, M. J., & Cox, P. 1996, in preparation
Skinner, C. J., Tielens, A. G. G. M., Barlow, M. J., Justtanont, K. 1992, ApJ, 399, L79
Smardzewski, R. R. 1978, J. Chem. Phys. 63, 2878
Smith, R. J., Sellegren, K., & Tokunaga, A. T. 1989, ApJ, 344, 413
Sofia, U. J., Cardelli, J. A., & Savage, B. D. 1994, ApJ, 430, 650
Strazzulla, G., & Baratta, G. A. 1992, A&A, 266, 434
Tielens, A. G. G. M. 1989, in IAU Symp. 135, Interstellar Dust, ed. L. J. Allamandola & A. G. G. M. Tielens (Dordrecht: Reidel), 239
Tielens, A. G. G. M., & Allamandola, L. J. 1987a, in Physical Processes in Interstellar Clouds, ed. G. E. Morfill & M. Schoeler (Dordrecht: Reidel), 333
———. 1987b, in Interstellar Processes, ed. D. J. Hollenbach & H. A. Thronson (Dordrecht: Reidel), 397
Tielens, A. G. G. M., & Hagen, W. 1982, A&A, 114, 245
Tielens, A. G. G. M., Tokunaga, A. T., Geballe, T. R., & Baas, F. 1991, ApJ, 381, 181
van Steenbergen, M. E., & Shull, J. M. 1988, ApJ, 330, 942
Whittet, D. C. B., & Duley, W. W. 1991, A&A Rev., 2, 167
Willner, S. P., et al. 1982, ApJ, 253, 174